



ELSEVIER

Contents lists available at SciVerse ScienceDirect

Journal of Quantitative Spectroscopy & Radiative Transfer

journal homepage: www.elsevier.com/locate/jqsrt

Investigation of fine and coarse aerosol contributions to the total aerosol light scattering: shape effects and concentration profiling by Raman lidar measurements

A. Quirantes^{a,*}, F.J. Olmo^{a,b}, H. Lyamani^{a,b}, A. Valenzuela^{a,b}, L. Alados-Arboledas^{a,b}

^a Departamento de Física Aplicada, Universidad de Granada, Fuentenueva s/n, 18071 Granada, Spain

^b Centro Andaluz de Medio Ambiente (CEAMA), Avda. del Mediterráneo s/n, 18071, Granada, Spain

ARTICLE INFO

Article history:

Received 21 March 2012

Received in revised form

1 August 2012

Accepted 2 August 2012

Keywords:

Nonspherical particles

Dust properties

T-matrix

ALFA database

AERONET

ABSTRACT

Remote sensing techniques, such as sun-photometry (columnar integrated aerosol parameters) and Raman lidar (profile aerosol parameters), are used in inversion models to yield information about particle size distribution (PSD), concentration, and average refractive index (RI). Ground-based AERONET network uses sun-photometric measurements to retrieve columnar effective particle size distribution and refractive index values, as well as other radiative properties such as absorption optical depth, albedo, and asymmetry parameter, which do not have a strong dependence on particle shape. Raman lidar measurements, on the other hand, yield shape-dependent quantities like particle depolarization, backscattering and lidar ratio at several wavelengths. In order to evaluate what light scattering parameters can be used to infer information regarding particle shape and concentration, a set of computer simulations was carried out. AERONET-inverted particle data (PSD, RI, concentration) have been used as input. Simulated data are obtained from ALFA, a light-scattering database, using the kernel approximation scheme. As expected, the effect of fine mode particle shape on near-infrared (1064 nm) was found to be negligible; on the other hand, even a small amount of nonsphericity in small particles has a marked effect on depolarization ratio values. Data from a 2007 lidar campaign were then used to evaluate the validity of our approach on a real measurement campaign. Results show that our method can yield some information about layer profiling, such as the concentration of fine mode particles. Such information comes not as a best-fit solution but in the form of a compatible set of possible solutions, which could be narrowed by the use of closure relations.

© 2012 Published by Elsevier Ltd.

1. Introduction

Coarse mode scatterers, such as mineral and dust particles, play an important role in the Earth's radiation budget, being responsible for about one-third of global aerosol extinction optical depth [1]. The long-range transport of

mineral particles by the combined action of convection currents and general circulation systems make them a significant aerosol constituent even at locations far from their sources [2]. North African dust from the Sahara desert is carried across the Mediterranean basin to Europe and the Middle East, and, across the Atlantic Ocean, to the Caribbean and the southeastern United States. Large dust sources can also be found in India (Thar desert), China (Taklamakan desert), the African Sahel (Bodele depression), etc.

In these cases, dust aerosols are not to be found alone. As they are injected in the atmosphere, and then

* Corresponding author. Tel.: +34 958240019; fax: +34 958243214.

E-mail addresses: aquiran@ugr.es (A. Quirantes), fjolmo@ugr.es (F.J. Olmo).

transported to other regions, they can form a mixture with other particles produced in combustion process (forest fires, fossil fuel combustion, biomass burning, urban traffic) [3]. The mixing of desert dust with anthropogenic particles may prompt changes in its physical properties [4] and this may have important consequences in processes affecting climate [5]. The resulting particle size distribution (PSD) could be described as a mixture of a submicron-sized fine mode of combustion-produced particles, and a micron-sized coarse mode of dust particles. Coarse particle outburst of a different origin forced the closure of the European airspace, when the Icelandic Eyjafjallajökull volcano erupted in 2010. Its impact on flight safety depended heavily on its composition, and the distinction between ash and non-ash particles became a necessity [6].

Photometric measurements of solar extinction and sky radiance are used in inversion models to yield information on columnar-integrated aerosol particle size distribution, particle concentration, refractive index, single scattering albedo, and asymmetry parameter [7,8]. Such inversions do not yield any information on particle shape, or on the refractive index of either mode (an average value is given). Neither does it include other light-scattering parameters such as backscattering, particle depolarization ratio, or liar ratio (extinction to backscattering ratio); parameters of great potential value in particle characterization, as they are highly dependent on particle shape. Multi-wavelength liar, on the other hand, allows for an independent calculation of aerosol extinction and backscattering coefficients profiles, together with particle depolarization ratio. Microphysical properties of particles have been obtained from remote sensing techniques by assuming spherical particles, with some degree of success [9], but the effect of particle shape cannot be discarded in some parameter like backscattered particle depolarization ratio, even at small particle size. Veselovskii et al. [10] recently adopted the AERONET inversion concept with the inclusion of a spheroidal model in the liar retrieval of aerosol physical properties. Lidar and sunphotometry data from AERONET and EARLINET have also been combined to retrieve vertically resolved properties of fine and coarse mode aerosols [11]

In the present paper, an attempt is made to separate fine and coarse mode contributions to the total aerosol light scattering. In the first part, the effects of shape and concentration have been simulated on a two-mode particle size distribution, with the goal of assessing what light scattering parameters are most sensitive to particle shape and concentration. The second part shows the results of a method to obtain columnar, and layer-by-layer, information on particle concentration based on their extinction and backscattered signals. This would allow the evolution of aerosol dust episodes, including layer mixing, to be followed from in-situ measurements.

2. Methods

Computer simulations were carried out by using the *T*-matrix method under the assumption of randomly oriented, axially symmetric scatterers [12]. In order to

ease the burden of computation for each simulation, our approach was to pre-calculate a database containing light scattering data from all potential particle parameters (size, shape, and composition). Such database, code-named ALFA [13], currently includes information for the following kind of particles:

- Index of refraction, real part m_r : 1.33–1.6 (15 values)
- Index of refraction, imaginary part m_i : 0.0005–0.64 (30 values)
- Shape ε : oblate and prolate spheroids with axial ratio values 1.0–3.0 (21 values)
- Equivalent-volume-sphere size parameter x_{eq} : 0.01 to a shape-dependent maximum value (up to 140 for $\varepsilon=1.2$, or 20 for $\varepsilon=3.0$).

Index of refraction values and size parameter is logarithmically spaced, both the real and the imaginary part; likewise for size parameter values. The reason why the maximum size parameter is different for each shape derives from the well-known fact that *T*-matrix calculations become unstable for large particles, and the maximum size for which convergence is achieved drops with increasing departure from nonsphericity. The use of RES (Spanish Super-computation Network) resources allowed us to extend calculations to quadruple-precision accuracy, which helps (but not completely) in increasing the maximum size for which calculations can be successfully achieved.

The current size of ALFA(92 GB, and growing) is uncomfortably high for practical applications, and its direct use requires a considerable computer time usage. For that reason, and following suggestions by Dubovik et al. [8], single-scattering properties of particles can be approximated as a sum of so-called kernel functions. Starting from ALFA, a set of kernel functions has been built, yielding a second database (“BETA”) of smaller size, and easier to use. BETA has been used in this paper for comparison between theoretical and experimental results.

Scattering particle populations have been modeled as a bimodal lognormal volume size distribution:

$$\frac{dV(r)}{d\ln r} = \sum_{i=1}^2 \frac{C_{v,i}}{\sqrt{2\pi}\sigma_i} \exp\left[-\frac{\ln^2(r/r_{\text{mod},i})}{2\sigma_i^2}\right] \quad (1)$$

where $C_{v,i}$ is the volume concentration per unit lateral area for particle mode i (sub-indices 1,2 refer to fine and coarse mode, respectively). Particles for both modes (fine and coarse) have been simulated as an equal-volume mixture of randomly oriented prolate and oblate spheroids with the same axial (long-to-short axis) ratio ε . Values for $r_{\text{mod},i}$ refer to equivalent-volume-sphere radius.

3. Leipzig-based study

In order to rate the changes of light scattering parameters on particle shape and concentration, a particle size distribution from an experimental campaign has been chosen. The PSD chosen for our study matches that obtained from measurements at the IFT-Leipzig Station on 14:49 UTC, April 19, 2010. At that time, Leipzig was one of several AERONET stations monitoring the April 2010

Eyjafjallajökull volcanic eruption, which forced the closing of European airspace for several days. A full account of the measurement campaign and layer profiling can be found in [14].

For each mode (fine, coarse), a single value of ε has been considered from a set ranging from 1.0 to 1.8; the latter value is a good approximation to the average eccentricity of dust aerosols [15], while the former covers the case of spherical particles. The use of nonspherical shapes has greatly improved the retrieval of dust and volcanic properties [8,9]. Regarding the fine mode case, the usefulness of the spherical approximation has been proven on past applications where extinction or asymmetry parameters are dealt with (e.g. sunphotometry). However, the effect of the fine mode particle shape on the values of shape-sensitive quantities such as particle depolarization ratio values cannot be ruled out. In the Leipzig case, the modal radius for the fine mode is about $0.2\ \mu\text{m}$, which means a size parameter $x=2.4$ for a $532\ \text{nm}$ incident wavelength. The tail of the distribution includes about 1% of fine mode particles with size larger than $1\ \mu\text{m}$, a size for which depolarization ratio can reach large values [16]. Under such circumstances, the reader is warned that the assumption of perfect spherical shape could yield misleading values of the particle depolarization ratio; the use of nearly spherical scatterers would then be a better choice.

Values of the refractive index used for simulations are $m=1.459+i0.0036$ ($\lambda=532\ \text{nm}$), and $m=1.478+i0.0022$ ($\lambda=1064\ \text{nm}$), which closely resemble the refractive index data given by the AERONET inversion. Radius, width, and concentration values for the PSD are shown in Table 1.

Simulation results for several values of the axial ratio in both fine and coarse modes show a 75% variation observed in the backscattering coefficient at $532\ \text{nm}$, and a slightly lower value (65%) for $1064\ \text{nm}$ (Fig. 1). The backscattering coefficient ratio $\tau(532)/\tau(1064)$, or color ratio, shows a smaller variation (29%), with the highest value for a spherical fine mode and a highly nonspherical coarse mode. Lidar ratio (extinction to backscattering ratio) also changed within a 70% range from the smaller to the largest value, with increasing values as both fine and coarse mode particles departed further from sphericity (Fig. 2). It was found that lidar ratio values for $\lambda=1064\ \text{nm}$ are insensitive to the value of the fine mode's axial ratio, and could therefore be used as a useful observable to help determine the shape of the particles in the large (coarse) mode by assuming a constant value of the fine mode particle shape.

Depolarization ratio values also show a large dependence on shape, with differences of up to 160% for $532\ \text{nm}$

Table 1

Particle size distribution parameters for the Eyjafjallajökull measurement (ITF-Leipzig Station, April 19, 2010, 14:39 UTC.

	Mode 1 (fine)	Mode 2 (coarse)
Concentration $C_{v,i}$ ($\mu\text{m}^3/\mu\text{m}^2$)	0.080	0.078
Modal radius $r_{\text{mod},i}$ (μm)	0.205	1.721
Width σ_i	0.485	0.631

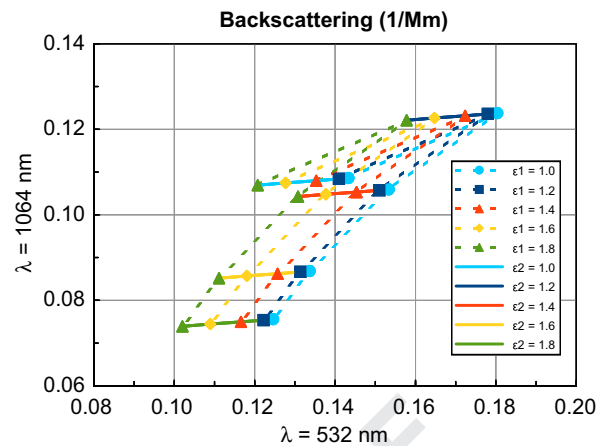


Fig. 1. Backscattering values at $\lambda=532, 1064\ \text{nm}$, for a PSD fitting AERONET data (ITF-Leipzig April 19, 2010) PSD values are given in Table 1.

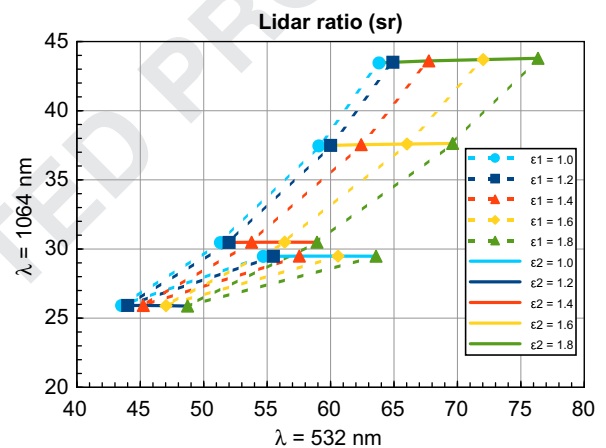


Fig. 2. Same as Fig. 1, for lidar ratio.

wavelength, and 57% for $1064\ \text{nm}$ when nonspherical particles are considered. Even nearly spherical scatterers ($\varepsilon=1.2$ have been found to make a substantial contribution to total depolarization, and that happens for both large and small particles. As Fig. 3 shows, fine and coarse mode particles with an axial ratio $\varepsilon_1=\varepsilon_2=1.2$ yield a value of nearly 16% for the degree of polarization at both wavelengths. It is known that the relationship between depolarization and size parameter is not systematic, and that small depolarization values can be obtained with large particles. The same applies to shape: particles close to sphericity can act as better depolarizers than highly aspherical ones [16–18]. The presence of a strong depolarization signal is not necessarily an indication of large shape departure from sphericity. The opposite also holds: small depolarization values does not imply that particle shape is predominantly quasi-spherical. This fact is of importance since “zero depolarization value” becomes a meaningless expression in real measurements, where experimental uncertainty is always present one way or another.

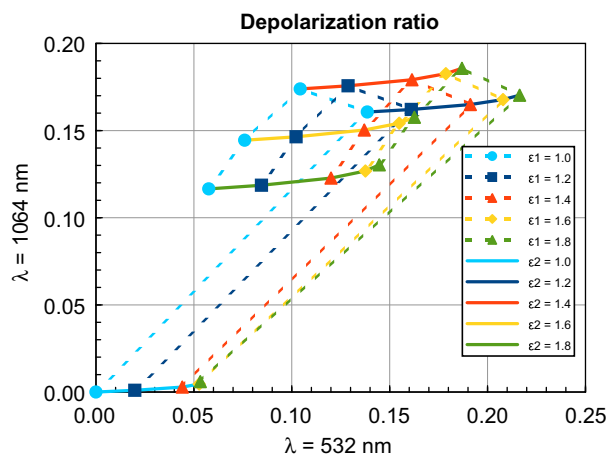


Fig. 3. Same as Fig. 2, for depolarization ratio.

In order to help make an assessment on whether backscattered light properties (e.g. lidar ratio, depolarization, Ångström exponent for backscattering) can be useful as a tool to quantify the contribution of fine and coarse modes to the PSD, the relative concentration of the fine mode (C_{rf}) was changed from 0 (full coarse mode) to 1 (full fine mode), while keeping the total volume concentration fixed to $0.158 \mu\text{m}^3/\mu\text{m}^2$. In both cases (532 and 1064 nm wavelengths), lidar ratio was found to rise with increasing fine mode concentration, sometimes in a lineal way. As Fig. 4 shows, a lidar ratio value for a single wavelength cannot be used to infer particle relative concentration unless the particle shape for both modes are known.

A look at the Ångström exponent for backscattering (Fig. 5) allows us to improve our knowledge of the possible fine mode fraction values. For example, a backscattering Ångström value of 0.5 yields a fine fraction range of 0.45–0.6, depending on particle shape. Backscattering measurements at two wavelengths can be therefore used to obtain a reasonable range of values for relative mode concentration. Color ratio curves also show a monotonic rise for increasing concentration of the fine mode. This suggests that, given a two-mode aerosol particle population, an increase or decrease in the relative presence of one of the two modes could be detected by corresponding changes in the color ratio.

Depolarization ratio values, shown in Fig. 6, do not seem to have a direct relationship with fine/coarse mode ratio, except for a general decrease in increasing fine mode concentration. Values at 1064 nm show little dependence on fine mode particle shape ϵ_1 , and for higher fine mode concentrations ($C_{rf} < 0.3$) a weak dependence on coarse mode particle shape ϵ_2 is also found. This is not the case for the 532 nm wavelength case, where a single depolarization ratio value can be associated to different fine mode values, depending on particle shape.

4. Granada layer profiling

To check the possible use of light-scattering measurements as a way to retrieve information on fine/coarse mode concentration values in a layer-by-layer case, a set

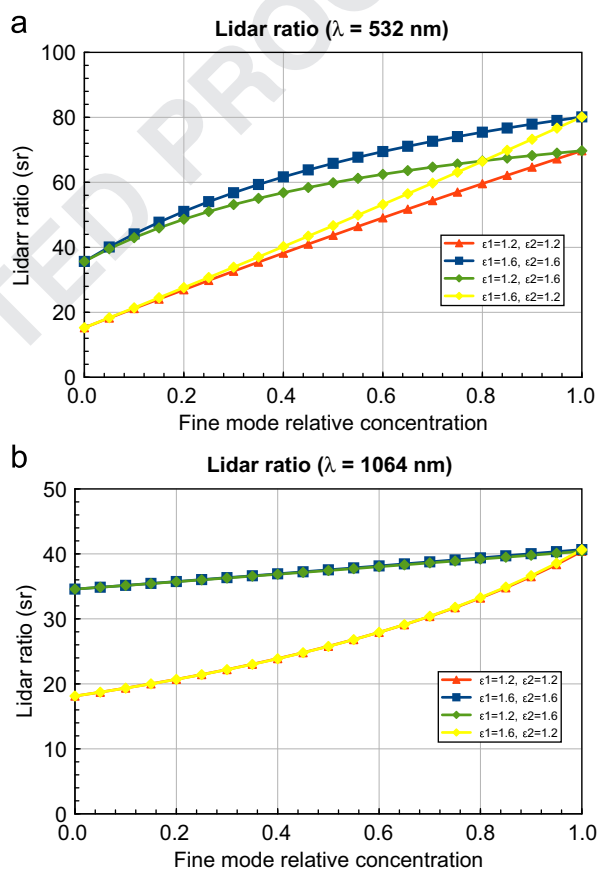


Fig. 4. Lidar ratio values at $\lambda = 532$ (a), 1064 nm (b), as a function of fine mode relative concentration (PSD data as Table 1).

of experimental data was used from an observation campaign of a fresh biomass-burning pollution plume over Granada, Spain (37.16°N 3.6°W , 24–25 September 2007). Aerosol optical depth was measured with an AERONET Cimel radiometer CE-318-4 [7]. A multiwavelength Raman lidar was used for vertically resolved measurements of backscattering (355, 532, 1064 nm)

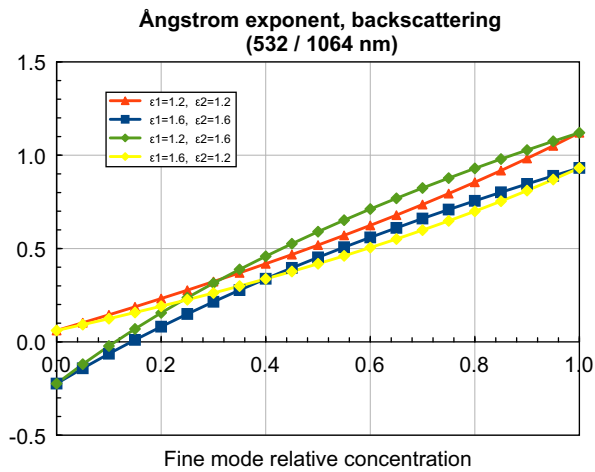


Fig. 5. Same as Fig. 4, for backscattering Ångström exponent.

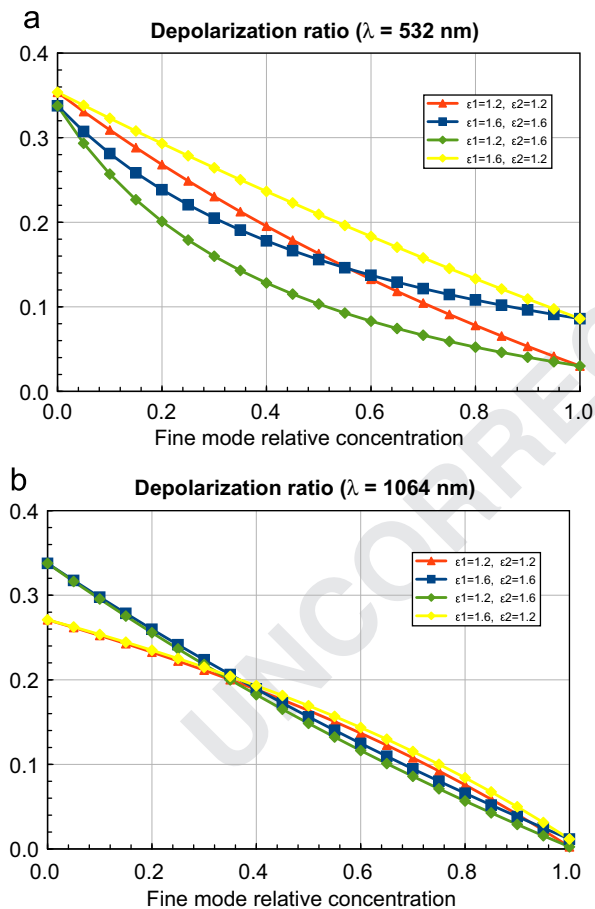


Fig. 6. Same as Fig. 5, for depolarization ratio.

and extinction (355, 532 nm) coefficients [19]. Values at three layers, measured at 19:03–20:03 UTC on September 24, are shown on Table 2. Depolarization ratio values were measured but were unreliable due to calibration problems so they will not be used in this test case. Uncertainty for each experimental value (extinction and

Table 2

Experimental data for the Granada biomass burning case, 24 September 2007, 19:30–20:03 UTC (by layer).

Layer km (a.s.l)	Backscattering (Mm ⁻¹ sr ⁻¹)			Extinction (Mm ⁻¹)	
	355 nm	532 nm	1064 nm	355 nm	532 nm
2.0–2.5	3.40757	2.30506	0.907132	219.08	141.059
2.5–3.0	2.57662	1.59019	0.622492	157.196	94.9235
3.0–3.5	1.52414	0.91195	0.362847	95.0378	56.4928

backscattering coefficients) is assumed in this paper to be 5% in all cases. PSD for both fine and coarse mode (modal radius, width concentration) are from AERONET data (Table 3). In order to compare results to AERONET inversion results, a single, average value of the index of refraction has been used for both modes.

For remote sensing applications, the choice of a particle shape distribution is considered as a better choice [20]. Scatterers such as desert dust aerosols typically lack spherical shapes, while sphericity (rather, near sphericity) seems to be the usual shape for maritime aerosols. In our case (biomass burning), aerosol shows nearly constant shape distribution [8]. In the present work, no particular shape distribution is assumed, except that a given PSD for an given axial ratio includes the same volume of oblate and prolate particles.

The question we intended to answer was assumed a known, bimodal PSD, with an average refractive index for both modes, is there a single set of shape/composition parameters (ϵ_1 , ϵ_2 , m) which fits experimental data (backscattering, extinction) to within experimental uncertainty? The simple answer is no. Using size/shape parameters from the BETA kernel database, a discrete set of 297 valid solutions was obtained for shape parameter values ranging from 1.0 to 1.8. Depolarization measurements, highly dependent on shape, are not available for this simulation; in this case, spherical particles (ϵ_1 or ϵ_2 equal to 1) can be now considered as valid.

An error parameter was calculated for each solution, based on the differences between experimental and theoretical values. Such parameter could be used to choose the best-fit solution out of our discrete set of possible solutions. We chose not to use that approach for two reasons. First, as stated before, particle shape affects the backscattering values. A given value of the Ångström exponent for extinction would not yield an accurate value for the fine/coarse volume ratio unless particle shape is well known. Second, a best-fit parameter would be a reliable indication of good agreement between theory and experiment only if the measured light scattering magnitudes were error-free, which is usually not the case. It cannot be assumed that a particular theoretical fit is better than other on the basis of an best-fit parameter alone, as long as the basis for the fit is an experimental measurement which itself carries some degree of uncertainty. Therefore, all 297 solutions were considered as acceptable within experimental bounds.

A comparison of experimental and simulated data for both backscattering and extinction Ångström exponent is

given in Fig. 7. Each point represents the best-fit fine-mode concentration for a given solution (ε_1 , ε_2 , m). The maximum-likelihood index of refraction (the one that includes the largest number of possible solutions) is $m=1.56+i0.008$. The full set of solutions yields an average index of refraction value of $m=1.56+i0.007$, with a standard deviation of 0.04 for the real part and 0.004 for

Table 3

Particle size distribution parameters for the Granada biomass burning case, 24 September 2007, 19:30–20:03 UTC.

	Mode 1 (fine)	Mode 2 (coarse)
Concentration $C_{v,i}$ ($\mu\text{m}^3/\mu\text{m}^2$)	0.030	0.023
Modal radius $r_{\text{mod},i}$ (μm)	0.154	2.714
Width σ_i	0.433	0.656

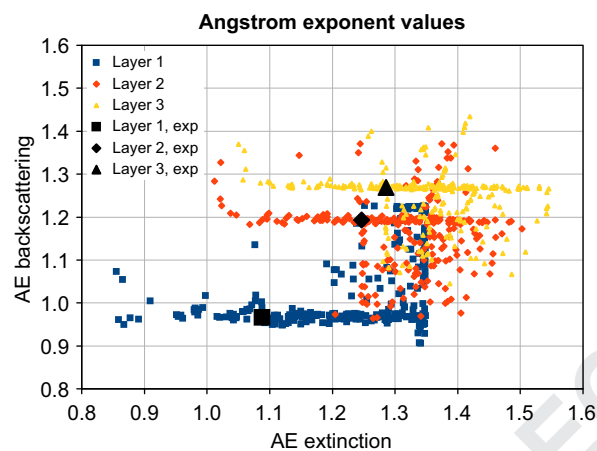


Fig. 7. Extinction and backscattering Ångström exponent values for all valid solutions to the Granada biomass-burning plume of September 24, 2007, 19:03–20:03 UTC (color) and experimental measurements (black), by layer. (For interpretation of the references to color in this figure legend, the reader is referred to the web version of this article.)

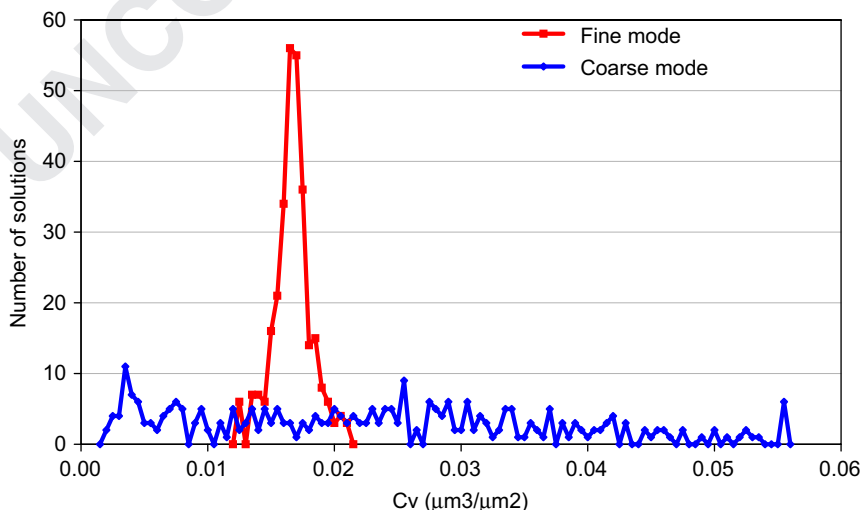


Fig. 8. Distribution of values for full (column-integrated) particle size concentrations for the solutions of Fig. 7. Red: fine mode, blue: coarse mode. (For interpretation of the references to color in this figure caption, the reader is referred to the web version of this article.)

the imaginary part. This is in close agreement to the values retrieved by Alados-Arboledas et al. [19] of $m=1.49+i0.02$ (layer 1) and $m=1.53+i0.02$ (layers 2 and 3); with uncertainty of ± 0.12 – 0.14 for the real part and 0.02 for the imaginary part. Average values for the Ångström exponent fit experimental data to within 5–13% for extinction, and 2–6% for backscattering, a percentage lower than the standard deviation of simulated data in all cases but one (Ångström exponent, layer 1).

Concentration values retrieved vary from one solution to another. Still, some information can be obtained. Fig. 8 shows that the full (column-integrated) concentration is nearly constant for the fine mode, with an average value of $C_{v,1}=0.017 \mu\text{m}^3/\mu\text{m}^2$. Coarse mode concentration values move in a large range, with an average of $C_{v,1}=0.023 \mu\text{m}^3/\mu\text{m}^2$. These data compare to those obtained by column-integrated Cimel values (0.030 and $0.023 \mu\text{m}^3/\mu\text{m}^2$, respectively). The lower value for the fine mode value could be partly explained by the fact that only three layers were considered, ranging from 2 to 3.5 km, and therefore fine mode particles at lower layers have only been accounted for in column-integrated measurements.

Fig. 9 shows the relative concentration of particles by layer. As seen, the total concentration decreases with increasing altitude. In addition, the contribution of the average coarse mode to average total concentration also decreases with altitude: 65% (2.0–2.5 km), 52% (2.5–3.0 km), and 42% (3.0–3.5 km). This trend is in agreement with measurements made by Alados-Arboledas et al. [19], where data regarding effective radius seem to show an downward trend at higher altitudes: 0.17, 0.15, and $0.13 \mu\text{m}$, respectively. It must be pointed out, however, that uncertainty in the effective radii does not make this trend significant.

This simulation has also shown us where improvements are due to the narrow range of possible solutions, and to improve its accuracy. Fine and coarse particles are typically made up of different particles (soot and dust, for instance), which calls for two different values of the

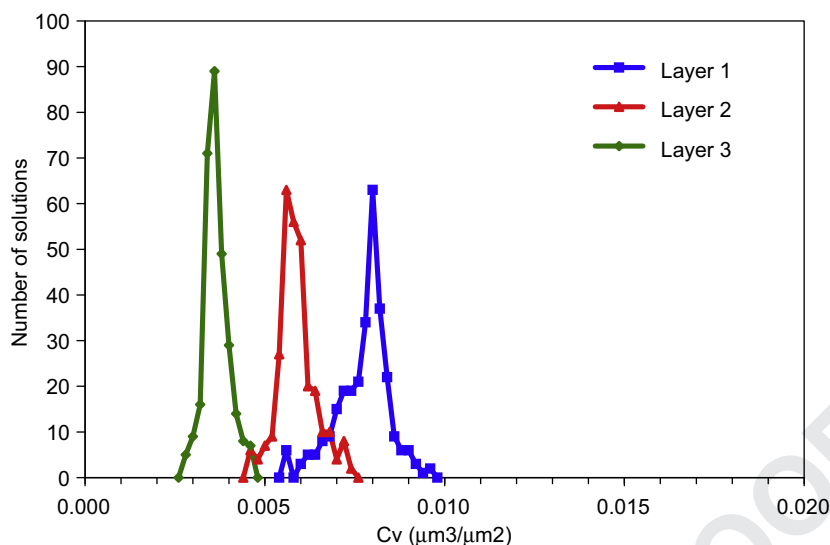


Fig. 9. Distribution of values for layer-by-layer fine mode particle size concentration for the solutions of Fig. 7.

refractive index. Additional steps to improve the quantity and quality of results include accurate measurements of depolarization ratio values and its use as fitting parameters; multiwavelength measurements; and a wide range of shape and refractive index for computer simulations. The use of closure relations could help rule out some solutions; as an example, the added concentration given by all layers should not be larger than that given by the Cimel column-integrated data.

5. Conclusions

Light-scattering parameters depend on particle size, shape, and composition in a very complex way. Some quantities show little dependence on shape, (e.g. extinction optical depth, single-scattering albedo), while those related to backscattering light, are more sensitive to both shape and relative concentration. Results in this paper give us a hint of which parameter can be best put to use in order to determine either shape or relative concentration in a two-modal population of soot/dust particles. This is particularly useful in lidar measurements, where shape-dependent experimental data such as depolarization and backscattering can be obtained for a set of horizontal layers. Relative distribution of particles by layer could be determined from backscattered light measurements, and thus a separation of fine and coarse mode could be made. This approach is similar to that of Tesche et al. [21]. In a particular layer, the concentration value for the fine mode can be approximately retrieved, but the coarse mode has a wide margin of uncertainty. Even for a particular value of shape and index of refraction parameters, however, relative concentration values for both fine and coarse modes can only be obtained as a range of plausible values, since simulations are compared to experimental data which always has a degree of uncertainty. Possible solutions should be treated not as best-fit-only but as a distribution

of compatible aerosol ensembles, as suggested by Gasteiger et al. [6].

Acknowledgment

This work was supported by the Andalusian Regional Government through projects P08-RNM-3568 and P10-RNM-6299; by the Spanish Ministry of Science and Technology through projects CGL2008-01330-E/CLI (Spanish Lidar Network), and CGL2010-18782; by EU through ACTRIS project (EU INFRA-2010-1.1.16-262254); and by EARLINET-ASOS project (EU-CA, 025991, RICA).

The authors thankfully acknowledges the computer resources, technical expertise and assistance provided by the Barcelona Supercomputing Center. ALFA database computation was partly supported by RES (Spanish Super-computation Network) computing resources (projects AECT-2009-1-0012, AECT-2011-3-0016)

References

- [1] Tegen I, Hollrig P, Chin M, Fung I, Jacob D, Penner J. Contribution of different aerosol species to the global aerosol extinction optical thickness: estimates from model results. *J Geophys Res* 1997;102(D20):23895–4915.
- [2] Satheesh SK, Moorthy KK. Radiative effects of natural aerosols: a review. *Atmos Environ* 2005;39:2089–110. <http://dx.doi.org/10.1016/j.atmosenv.2004.12.029>.
- [3] Eck TF, et al. Climatological aspects of the optical properties of fine/coarse mode aerosol mixtures. *J Geophys Res* 2010;115:D19205. <http://dx.doi.org/10.1029/2010JD014002>.
- [4] Bauer S, Bierwirth E, Esselborn M, Petzold A, Macke A, Trautmann T, et al. Airborne spectral radiation measurements to derive solar radiative forcing of Saharan dust mixed with biomass burning smoke particles. *Tellus* 2011;63:742–50. <http://dx.doi.org/10.1111/j.1600-0889.2011.00567.x>.
- [5] Rodriguez S, Alastuey A, Alonso-Perez S, Querol X, Cuevas E, Abreu-Afonso J, et al. Transport of desert dust mixed with North African industrial pollutants in the subtropical Saharan Air Layer. *Atmos Chem Phys Discuss* 2011;11:8841–92.

- 1 [6] Gasteiger J, Gross S, Freudenthaler V, Wiegner M. Volcanic ash from
Iceland over Munich: mass concentration retrieved from ground-
3 based sensing measurements. *Atmos Chem Phys* 2011;11:2209–23.
<http://dx.doi.org/10.5194/acp-11-2209-2011>.
- 5 [7] Holben BN, et al. AERONET - A federated instrument network and
data archive for aerosol characterization. *Remote Sens Environ*
1998;66:1–16 doi: 10.1016/S0034-4257(98)00031-5.
- 7 [8] Dubovik O, et al. Application of spheroid models to account for
aerosol particle nonsphericity in remote sensing of desert dust.
9 *J Geophys Res* 2006;111:D11208. <http://dx.doi.org/10.1029/2005JD006619>.
- 11 [9] Veselovskii I, Kolgotin A, Griaiznov V, Müller D, Franke K, Whiteman
D. Inversion of multi-wavelength Raman lidar data for retrieval of
13 bimodal aerosol size distribution. *Appl Opt* 2004;43:1180–95.
<http://dx.doi.org/10.1364/AO.43.001180>.
- 15 [10] Veselovskii I, et al. Application of randomly oriented spheroids for
retrieval of dust particle parameters from multiwavelength lidar
17 measurements. *J Geophys Res* 2010;115:D21203. <http://dx.doi.org/10.1029/2010JD014139>.
- 19 [11] Chaikovsky AP, Dubovik O, Holben BN, Bril AI. Methodology to retrieve
atmospheric aerosol parameters by combining ground-based measure-
21 ments of multi-wavelength lidar and sun sky-scanning radiometer.
Eighth international symposium on atmospheric and ocean optics,
23 Proceedings of SPIE Vol. 4678 (2002).
- [12] Mishchenko MI. Light scattering by randomly oriented axially
25 symmetric particles. *J Opt Soc Am A* 1991;8:871–879;9:497
(errata).
- [13] Quirantes A, Olmo FJ, Valenzuela A, Lyamani H, Alados-Arboledas
L. ALFA/BETA: a dual database for light scattering simulations on
atmospheric aerosols. RECTA 2010 – IV Reunión Española de
Ciencia y Tecnología del Aerosol; Granada, Spain, 2010.
- [14] Ansmann A et al. Ash and fine-mode particle mass profiles from
EARLINET-AERONET observations over central Europe after the
eruptions of the Eyjafjallajökull volcano in 2010. *J Geophys Res*
2011;116:D00U02 10.1029/2010JD015567. 27
- [15] Müller D, et al. Mineral dust observed with AERONET Sun
29 photometer, Raman lidar, and in situ instruments during SAMUM
2006: shape-dependent particle properties. *J Geophys Res* 2010;
115:D11207. <http://dx.doi.org/10.1029/2009JD012523>. 31
- [16] Mishchenko MI, Sassen K. Depolarization of lidar returns by small
ice crystals: an application to contrails. *Geophys Res Lett* 1998;25:
309–12. 33
- [17] Mishchenko MI, Hovenier JW. Depolarization of light backscattered
by randomly oriented nonspherical particles. *Optics Letters* 1995;
20:1356–8. 35
- [18] Bohren CF, Huffman DR. Absorption and scattering of light by small
particles. New York: Wiley; 1983. 37
- [19] Alados-Arboledas L, Müller D, Guerrero-Rascado JL, Navas-Guzmán
F, Pérez-Ramírez D, Olmo FJ. Optical and microphysical properties
of fresh biomass burning aerosol retrieved by Raman lidar, and
star- and sun-photometry. *Geophys Res Lett* 2011;38:L01807,
<http://dx.doi.org/10.1029/2010GL045999>. 39
- [20] Mishchenko MI, Travis LD, Kahn RA, West RA. Modeling phase
functions for dustlike tropospheric aerosols using a shape mixture
of randomly oriented polydisperse spheroids. *J Geophys Res* 1997;
102:16831–47. 41
- [21] Tesche M et al. Vertically resolved separation of dust and smoke
over Cape Verde using multiwavelength Raman and polarization
lidars during Saharan Mineral Dust Experiment 2008. *J Geophys
Res* 2009;114:D13202 10.1029/2009JD011862 (2009). 43
45
47
49